Experimental Studies of Strong Hall Effects and U x B Induced Ionization

JAMES KLEPEIS* AND RICHARD J. ROSA†
Avco Corporation, Everett, Mass.

Using a graphite inert gas heater, many different MHD-generator channel and electrode configurations were tested. Typical flow conditions were 100 gm/sec argon at 1 atm pressure seeded with 0.1 to 1.0 mole-percent cesium vapor at 1800 to 2000°K. The aim of the work was to study MHD channel and electrode performance at high values of the Hall parameter (5 to 15) and to look for the occurrence of extra-thermal ionization. Straight segmented-electrode channels did not perform well, apparently due to a nonuniformity created by extrathermal ionization over the electrode walls. A disk geometry in which the current in the U × B direction closes upon itself performed much better. Enhancement of the power output due to U × B induced ionization was observed. The results correlate well with those obtained in applied electric field experiments and with theory when energy loss due to radiation is included. However, an instability was also observed when large increases in ionization were sought.

I. Introduction

MAGNETOHYDRODYNAMIC (MHD) devices, such as generators, have been operated with combustion gases at close to ideal performance[1] when the Hall parameter $\omega\tau < 3$ (ω is the electron cyclotron frequency and τ the electron mean free time). In the future, and in particular for adaptation to nuclear heat sources, the use of inert gases and efficient operation at higher values of $\omega\tau$ is apt to be desired. For example, if the working fluid is a noble gas seeded with an alkali metal, operation at high $\omega\tau$ can lead to the production of extra-thermal or nonequilibrium ionization.[2] However, as pointed out in Ref. 3, for $\omega\tau \gg 3$ effects such as gas nonuniformities may severely limit the performance of MHD generators or accelerators. The experiments described in this paper were undertaken in order to study MHD-generator channel and electrode performance at high $\omega\tau$ (5 to 15), and in the presence of nonequilibrium effects.

At a temperature of 1800 to 2000°K and at near atmospheric pressure, a mixture of argon and 0.1 to 1.0 mole-percent cesium vapor will provide a gas with 1) an $\omega\tau$ of 5 to 15 for applied magnetic fields in the vicinity of 10 K gauss and 2) an electrical conductivity greater than 1 mho/m.

The graphite heater employed for the experiments is described in detail elsewhere.[4]

II. Straight Channel Experiments

A. Electrode Geometry

Initial efforts were concentrated on straight channels with segmented electrodes because of an interest in studying electrode performance and because such channels have a lower surface-to-volume ratio than a disk or coaxial geometry (Fig. 1).

The first problem faced in a small (characteristic length 5 cm) MHD experiment is that unless electrode drop is minimized, electrode emission phenomena will mask volume processes that are of primary interest. We have found that an electrode drop of essentially zero can be achieved if the electrode is a wire that projects through the boundary layer and is in good contact with, and heated by, the hot gas stream. It is probably essential that the electrode be coated with alkali metal to get emission at the gas temperature at which we operate (1800 to 2000°K). However, we have not

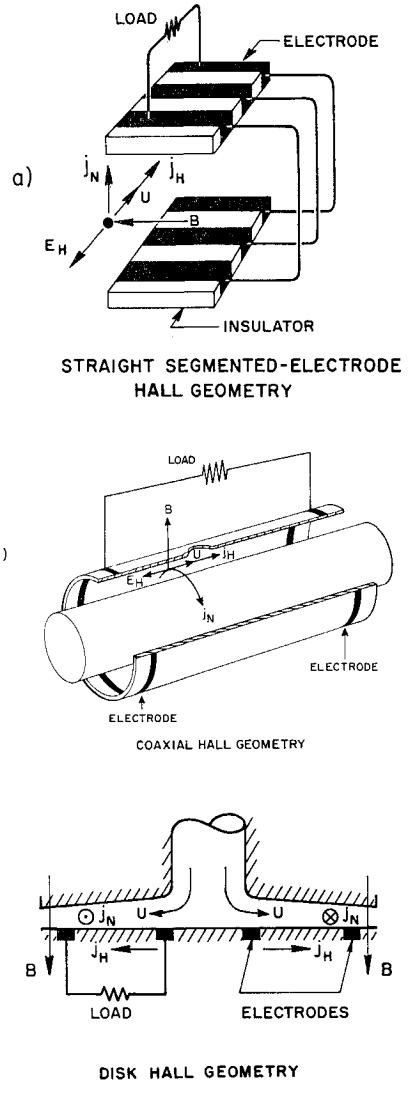

Fig. 1 Three kinds of Hall generator geometries.

Received December 16, 1964; revision received June 10, 1965. This work was partially supported by Headquarters, Ballistic Systems Division, Air Force Systems Command, U. S. Air Force, under Contract Nos. AF 04(964)-33 and AF 04(694)-414.

* Research Associate, Avco-Everett Research Laboratory. Member AIAA.

† Principal Research Scientist, Avco-Everett Research Laboratory. Member AIAA.

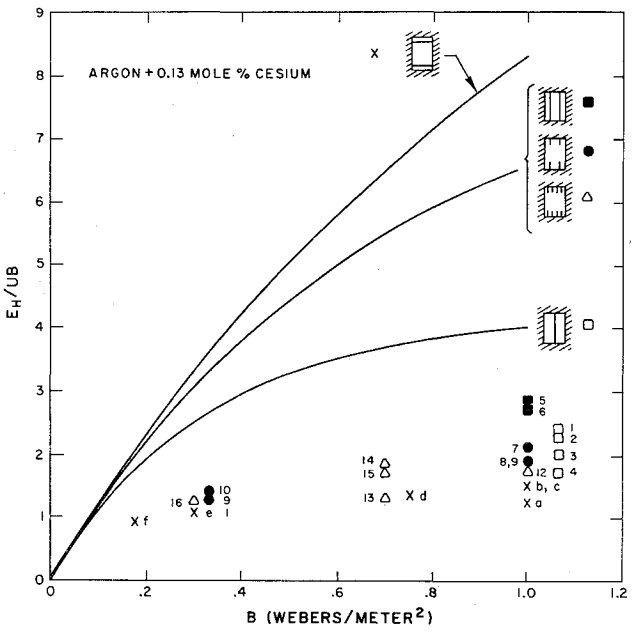

Fig. 2 Comparison between theory and experimental measurements of open-circuit Hall voltage in various straight segmented electrode Hall generators.

tried to separate this effect from the sudden increase in gas conductivity that also occurs when alkali seed injection starts. An electrode that was heated electrically, but did not project through the boundary layer, gave poor performance.

The drawbacks to a projecting wire electrode are the introduction of aerodynamic losses and local Hall effects. Theoretical analysis[5] indicates that these Hall effects [due to electrodes that project into the stream but have infinitely fine spacing in the longitudinal (flow) direction] will reduce generator power density by the factor

$$1/[1 + (w/2h)\omega\tau]$$

where w is the channel width and h the channel height. A similar factor applies for finite longitudinal spacing of the electrodes[6] ("segmenting"). The assumption is made that the real three-dimensional situation is described by taking the product of these two-dimensional factors.

The types of wire-electrode designs tested and their expected performance are sketched in Fig. 2. Each sketch is a view of the channel in a plane perpendicular to the gas velocity U. Channel dimensions were $h = 3$ in., $w = \frac{1}{2}$ in., and a length of 2 in. In addition to any transverse spacing, the electrodes were also spaced longitudinally with a pitch d of approximately $\frac{1}{8}$ in. The channels were operated as "Hall generators" in that all opposed pairs of electrodes were short-circuited (see Fig. 1).

B. Data: Comparison with Theory

Electrode and channel performance were evaluated by measuring the longitudinal or Hall field E_H for different values of applied magnetic field B and then comparing with theory. The results are summarized in Fig. 2. For a Hall generator, E_H/UB is theoretically equal to $\omega\tau$ times the correction factor for finite longitudinal[6] and transverse[5] spacing of the electrodes.

The experimental data were obtained over a gas temperature range (1800 to 2000°K) where $\omega\tau/B$ is nearly a constant equal to 13 m^2/weber. As shown in Fig. 2, it was not possible to generate Hall fields much greater than twice UB, even with values of $\omega\tau$ greater than ten and very fine segmenting ($h/d \approx 24$). It has been suggested by Kerrebrock[7,8] that this is caused by the current concentrations that appear at the electrodes and over the insulator between electrodes at high $\omega\tau$. As a result, in gases where nonequilibrium ionization is expected (e.g., argon), such ionization will always occur first in a layer over the electrodes. Nonuniformities of this type lead to rapid deterioration of performance.[3]

The theory and method of calculation developed in Refs. 7 and 8 yield results that show fair agreement with our experiment as shown in Fig. 3. These calculations also suggest the existence of a stability boundary within which one might achieve limited but useful nonequilibrium effects. In particular,[8] the operation of channels with rather course segmentation ($h/d \approx 4$) at low $\omega\tau$ (<5) may result in the production of some useful freestream nonequilibrium. Experimentation along these lines has been initiated.[9]

C. Plasma Diagnostics

In the course of our efforts to obtain good electrode operation at high $\omega\tau$, and in spite of our failure to do so, we have begun to accumulate a body of useful basic information on the properties of seeded gases.

By making due allowance for the very large departures from ideal behavior that can occur at high $\omega\tau$, one can get reasonably accurate and independent measurements of electron density n_e [both equilibrium (cold) and enhanced (hot)], and of electron mean free time (see Appendix). We thus appear to have a better than average method for bulk plasma diagnosis. For example, when the opposed electrodes of a segmented electrode generator are short-circuited, one can deduce the electron density under the condition that should produce the maximum departure from equilibrium from the formula [see Appendix, Eq. (16)]:

$$n_e(\text{hot}) = j_N B/(eE_H) \tag{1}$$

where j_N is the current density in the (normal) $\mathbf{U} \times \mathbf{B}$ direction and e the electron charge.

If a longitudinal or Hall-current short circuit is now imposed, the total (normal plus Hall) current density will be reduced. Under these conditions a measurement of short-circuit Hall current will determine the equilibrium (cold) electron density. For large values of $\omega\tau$ the short-circuit Hall current is in fact numerically equal to the number of ions flowing through the duct per second. Determination of $\omega\tau$ can be made by measuring the ratio of Hall current to normal current when the generator is short-circuited in the Hall direction.

It is shown in the Appendix that these measurements are relatively insensitive to the presence of nonuniformities, elec-

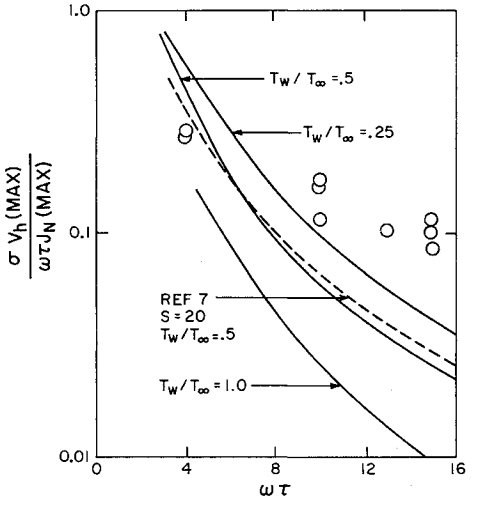

Fig. 3 Comparison of the theory described in Ref. 8 with our experimental results; T_w is the channel wall temperature, and S is the ratio of channel height to longitudinal electrode spacing.

trode effects, or other factors causing a departure from ideal behavior. Also, determination of scalar conductivity in the absence of a magnetic field affords checks both on the absolute values and on the internal consistency of the data. These methods all yield values averaged over the whole channel, rather than local values, but for many purposes this is satisfactory. Since we can make separate measurements of mean free time and of electron density we have for example a way of determining collision cross sections which is much more sensitive than are the usual measurements of conductivity alone (which measures the product $n_e\tau$). Figure 4 shows expected variations in electron density and mobility ($\omega\tau/B$) with seed concentration for several assumed argon and cesium collision cross sections. The experimental points indicate that 0.7 and 400 × 10^{-16} cm^2, respectively, are the proper choices for a Maxwell average at 2000°K. Strictly speaking, these experiments only measured the τ that determines $\omega\tau$, rather than the somewhat different "τ" that determines the conductivity. However, for MHD conversion the former is usually the quantity that one would like to know with the greatest accuracy.

Figure 5 shows a collection of experimentally determined values of cold electron density as a function of estimated stagnation temperature T_0 for different cesium seed concentrations. Good agreement with equilibrium theory based on stagnation temperature is obtained. The somewhat arbitrary but reasonable assumption was made that the gas stagnation temperature is 60°C less than the graphite-heater's core temperature measured with a pyrometer.[4] The local temperature, as calculated from a knowledge of Mach number, is also indicated in Fig. 5. It was found that the degree of ionization was fairly independent of the Mach number. On the basis of current electronic three-body recombination theories[10–12] this is to be expected. In the future, we will try to extend these measurements to T_0 = 2100°K and longer flow times. Departure from the stagnation values will then be observed provided the current recombination theories are correct.

III. Disk Generator Experiments

A. Early Results

To avoid the difficulties associated with finely segmented electrodes, channels of disk and coaxial shape (Fig. 1) have been tried. The latter has a difficult magnetic field configuration and so far no results of significance have been obtained. However, Hall voltages somewhat more than four times UB have been produced in the disk.

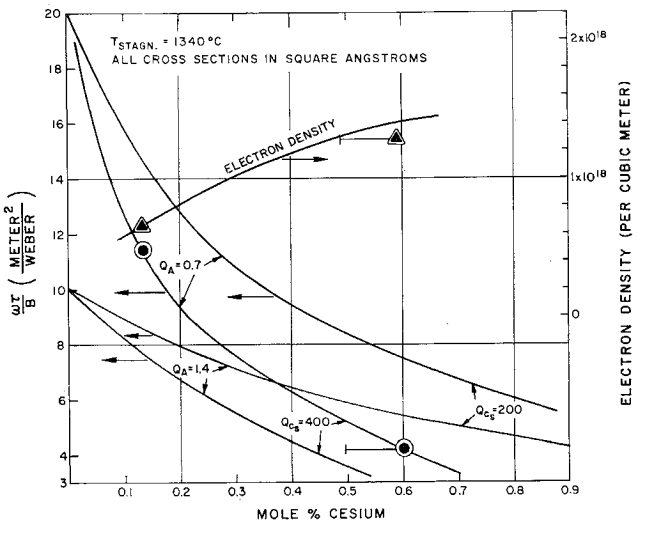

Fig. 4 Hall parameter and electron density vs seed concentration.

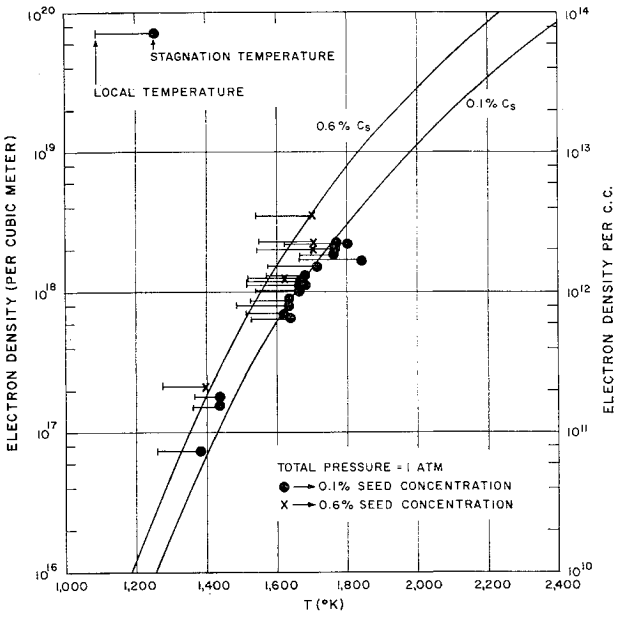

Fig. 5 Equilibrium (cold) electron density for argon plus cesium.

Typical disk dimensions (see Fig. 1) were a 3.6 and 1.6 in. diameter at the outer (anode) and inner electrode rings, respectively, and a constant, peripheral flow-area of 1.5 in.[2] The anode usually consisted of a ring of about 30 tungsten-wire "whiskers" connected to a single load resistance.

Figure 6 compares our disk results with theoretical calculations based on different amounts of variation of gas properties in the **U** × **B**, or normal, direction.[3] There are doubtless other property variations present in our experiment in addition to that assumed in the calculations. Thus the fact that our data falls close to the 80% "uniformity" curve suggests that we are getting performance nearly as good as can be expected at high $\omega\tau$. Although a larger device would probably do better, a high $\omega\tau$ machine will no doubt always show a larger deviation from ideal performance than a machine at low $\omega\tau$. Nevertheless we feel that these experimental re-

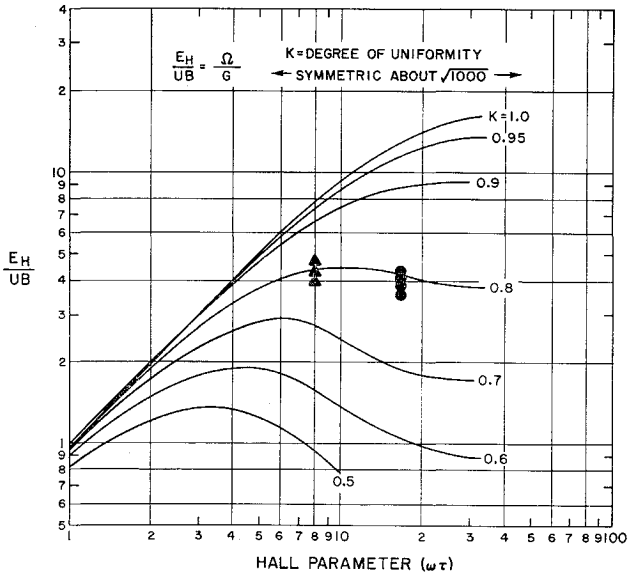

Fig. 6 Comparison of experimental Hall fields with theory for a nonuniform gas.[3] The degree of uniformity is defined as the ratio between the conductivity of alternate layers of gas. The curves are symmetric about $\omega\tau$ = $(1000)^{1/2}$.

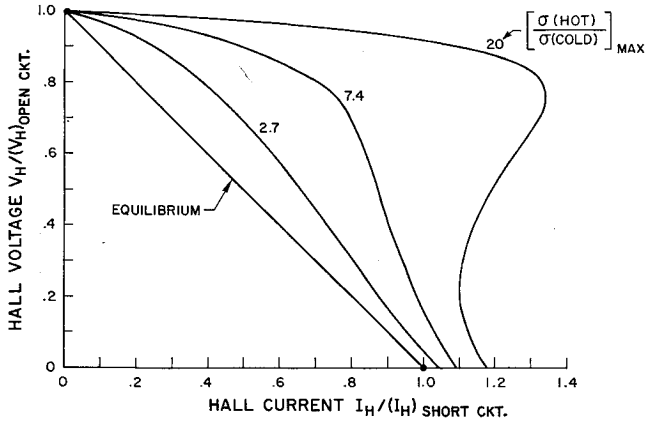

Fig. 7 Expected load lines for the disk Hall generator if nonequilibrium ionization occurs.

sults show that the prospects at high $\omega\tau$ are reasonably good for geometries in which the normal current closes within the gas. On the other hand these same geometries may be particularly susceptible to Hall instabilities or wave making processes such as are discussed in Ref. 13 and 14. We do observe a 10 to 15% a.c. component on the output Hall voltage which might become greater in a device of larger scale. It has been calculated that a pressure variation of only 1% could produce this result.[13] When displayed with time these fluctuations are quite irregular but seem to have a fundamental frequency of around 2.5 kc. This corresponds to a sound wavelength that is about equal to the circumference of the channel.

Many oscilloscope traces of the Hall voltage were obtained from two probes placed 90° from each other around the circumference of the disk. We have looked for differences in phase between the two signals in order to determine the velocity and direction of propagation of the waves and to see whether or not they reversed direction when the magnetic field was reversed. So far the results have not been consistent enough for one to draw any conclusions.

In Fig. 7, a series of expected load lines ($V_H \equiv$ Hall voltage, $I_H \equiv$ Hall current) for a Hall generator are sketched with the nonequilibrium to equilibrium conductivity ratio at open circuit $[\sigma\ (\text{hot})/\sigma\ (\text{cold})]_{\max}$ as a parameter. The shape of the expected curves at high values of this ratio is due to the fact that in a Hall-current generator the internal dissipation and hence the maximum departure from equilibrium is expected at open circuit. Note, however, that a Hall current greater than the equilibrium short-circuit value will never be observed unless the excess ionization is produced upstream of the section through which the Hall current is drawn, because this value of Hall current would prevent the ionization from ever building up. Thus a "two-stage" device is required to get an S curve with Hall current greater than the equilibrium short-circuit value. However, it has not been possible to incorporate this feature into our present device because of its small scale.

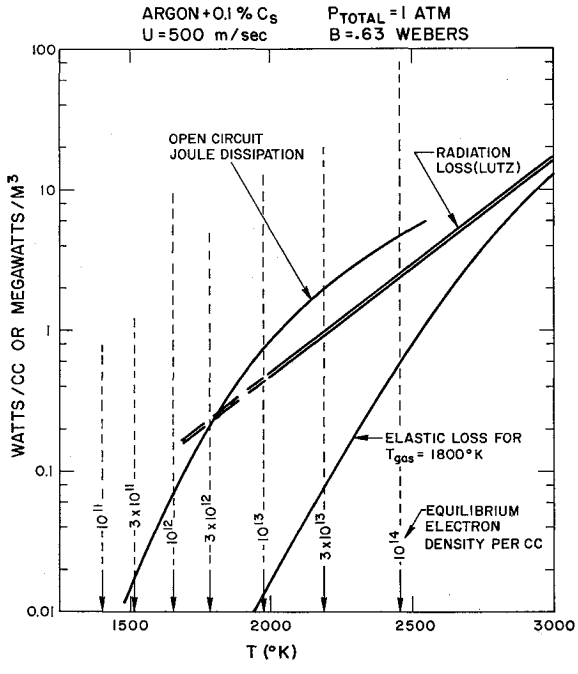

Fig. 8 Comparison of radiation loss and Joule dissipation.

Load lines for the disk channel were obtained by putting Hall voltage and Hall current on the y and x axis, respectively, of an x-y oscilloscope, and then photographing the trace obtained at many different load resistances. The gas used was argon seeded with 0.1 mole-percent cesium at stagnation temperatures between 1700 and 1800°K. Mach numbers were about 0.7, and the ideal $\omega\tau$ was approximately 8 (for a 6.3 K gauss applied magnetic field). For these early runs the equilibrium electron density was $<3 \times 10^{12}$/cc.

A fairly consistent feature of our early data was the slight negative curvature of the voltage-current trace. This implied the presence of some degree of nonequilibrium ionization, but not enough to make a noticeable improvement in the net power output. Abundant nonequilibrium should have been produced for the previously mentioned conditions if the electron velocity distribution had been Maxwellian and the only losses had been due to elastic collisions. However, the following makes it clear that this is not the case, at least in experimental apparatus of this size.

B. Radiation Losses and Nonequilibrium Ionization

Kerrebrock and Hoffman[15] have performed electric field ionization experiments with gas conditions and apparatus dimensions not too different from ours. Their measurements, which cover a wide range of currents, always resulted in voltage-current traces (Fig. 7 of Ref. 15) that exhibited a hump or voltage barrier before breaking over into the flat voltage characteristic typical of a nonequilibrium gas discharge. This barrier was observed occurring at an electron density of about 3×10^{12} per cc. They have proposed a number of possible contributing causes for this. Among these it seems clear that radiation loss plays a large role.

Figure 8 compares the open-circuit joule dissipation with estimated radiation loss in our experimental generator, based upon detailed calculations of line radiation loss by Lutz.[16] Also indicated is the elastic loss rate. Apparently our generator should *not* produce enough power to overcome radiation losses until an electron density of 3×10^{12}/cc is reached. In view of this we made a series of runs at successively higher values of inlet temperature and electron density. Typical results are shown in Fig. 9. The length of the line at any one load represents the a.c. component of the output. In order to see how far we were from obtaining $\mathbf{U} \times \mathbf{B}$ ionization, a voltage was applied which bucked the generated Hall field and reversed the flow of Hall current.

Observe that in Fig. 9a field ionization appears to occur at a negative Hall current about equal to the positive short-circuit value. In Fig. 9b it appears to occur at open circuit. In Fig. 9c which is at an electron density greater than 3×10^{12}/cc, clearly we have nonequilibrium ionization while operating as a generator.

At the point of maximum power output (which is near the "knee" of the curve in Fig. 9c) the conductivity appears to be about 4 times the equilibrium value and the power output between 2 and $2\frac{1}{2}$ times the maximum expected at thermal equilibrium (for the same degree of uniformity). If the shape of the voltage-current curve was entirely due to uniform changes in conductivity, the maximum conductivity en-

hancement inferred from Fig. 9c would be a factor of about 10 near open circuit.

This second point, however, is subject to considerable uncertainty. First of all observe on Fig. 10 that a large increase in conductivity above our starting point of about 10 mho/m will be accompanied by a significant drop in $\omega\tau$. This will also influence the shape of the curves. In particular we expect it to reduce the open-circuit Hall voltage. Because of the important but uncertain role played by nonuniformities it is

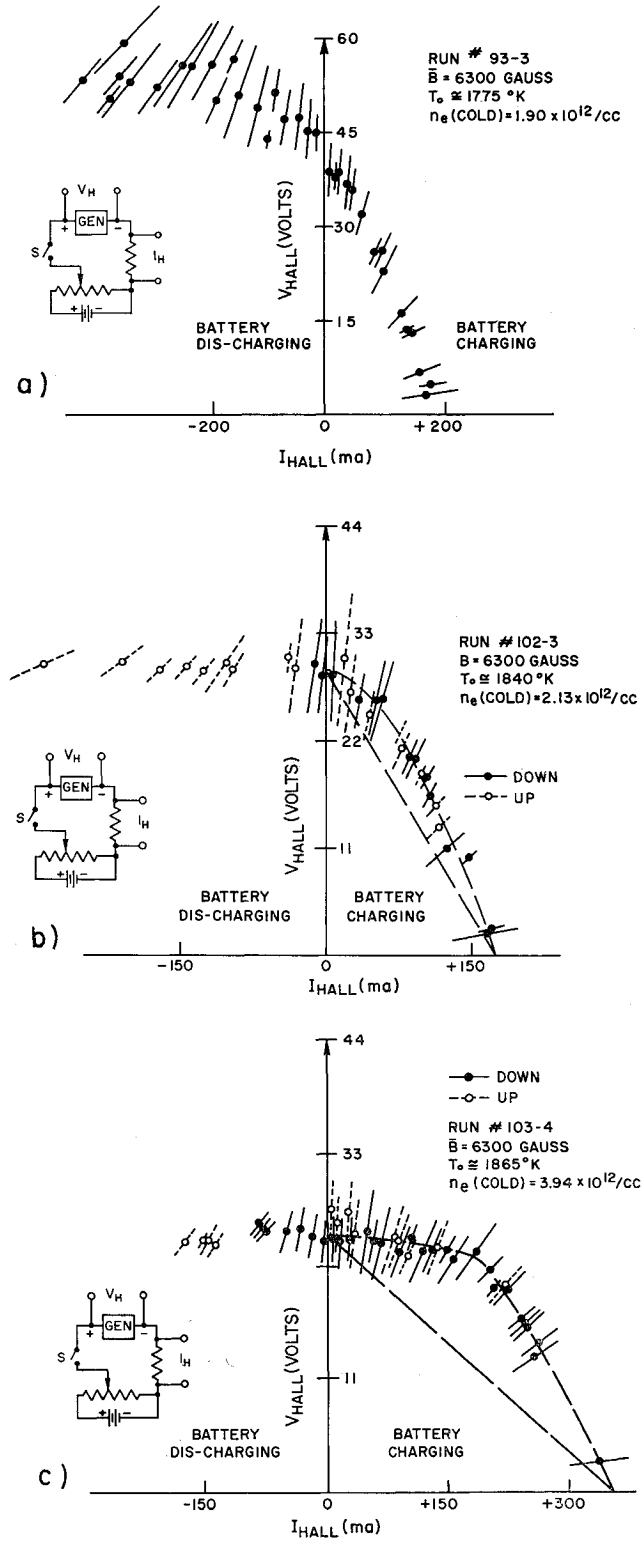

Fig. 9 Disk generator voltage-current characteristics for successively higher stagnation temperatures. The cesium seed concentration in argon was about 0.1 mole %.

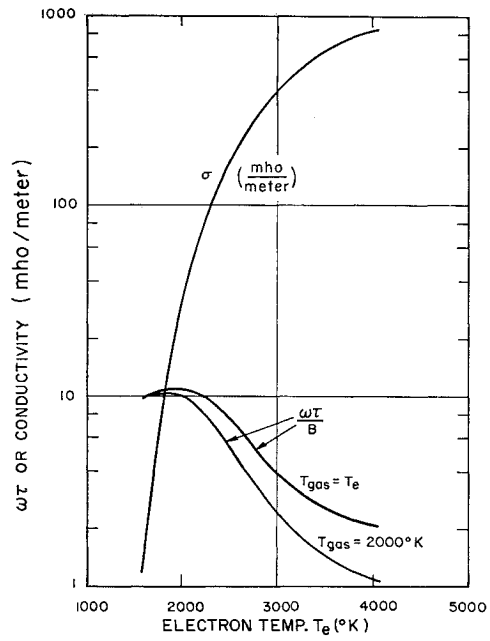

Fig. 10 Conductivity and Hall parameter for argon plus 0.175 mole % cesium.

difficult to predict how big this effect should be. Experimentally we observe that on the average, the open-circuit voltage obtained in high-current runs exhibiting nonequilibrium effects is approximately 20% lower than that obtained in low-current runs (Fig. 11). A change of this magnitude due to changes in $\omega\tau$ is not unreasonable.

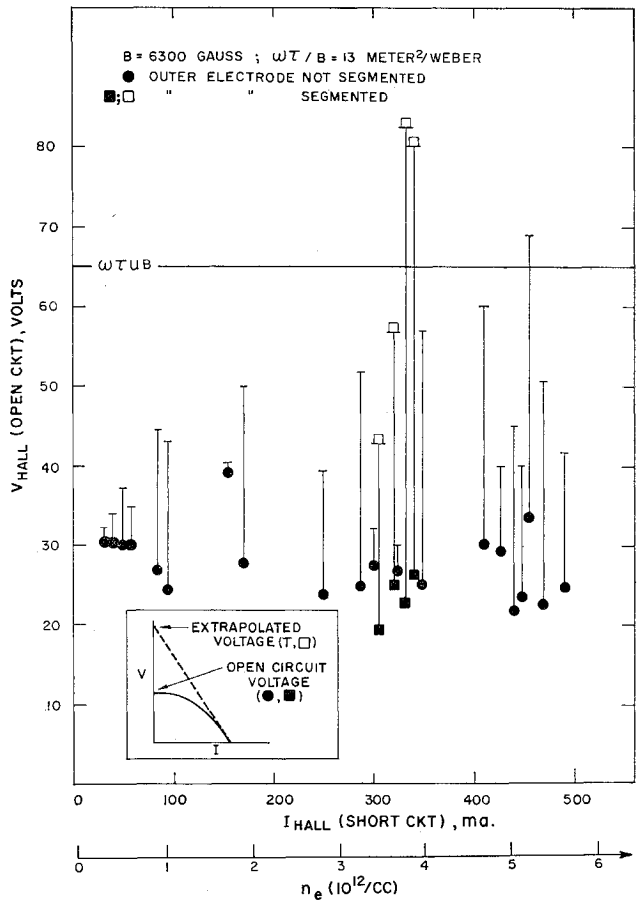

Fig. 11 Measured and extrapolated open-circuit Hall voltage for various short-circuit Hall current runs

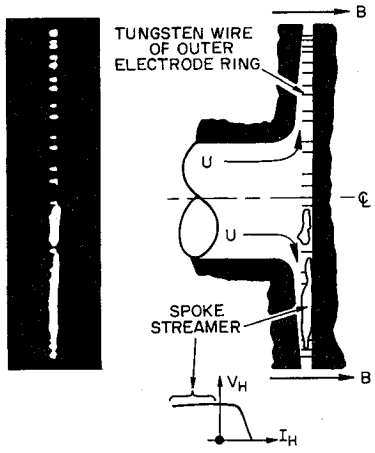

Fig. 12 Spoke streamer produced with a battery in the disk generator load circuit.

C. Ionization Instability

Another, and more important, effect has also been observed. Above the knee of the curves the ionization process gives every appearance of being unstable, resulting in longitudinal streamers, or in the case of the disk generator, what we might call ionization "spokes." These decrease the uniformity of the gas, and in effect partially short the Hall voltage. It can be shown mathematically that at high $\omega\tau$ there is a strong tendency toward longitudinal breakdown.

For a Hall-generator (i.e., normal electric field $E_N \equiv 0$), the equations for Hall and normal current densities (neglecting ion slip) are

$$j_H = \omega\tau\, j_N + \sigma E_H \tag{2}$$

$$j_N = \sigma U B - \omega\tau\, j_H \tag{3}$$

Consider the case of a Hall generator at open circuit. Then, if we designate all unperturbed or zero-order quantities by $(\ )_0$, $(j_H)_0 = 0$, and the unperturbed normal current is

$$(j_N)_0 = (\sigma)_0 UB \tag{4}$$

Putting these zero-order values in Eq. (2) gives

$$j_H = \omega\tau UB[(\sigma)_0 - \sigma] \equiv -\omega\tau UB\Delta\sigma \tag{5}$$

and

$$j_H/(j_N)_0 = -\omega\tau\Delta\sigma/(\sigma)_0 \tag{6}$$

The electron temperature or the dissipation per electron will be proportional to $(j/\sigma)^2$, where j is the total (normal plus Hall) current density. So

$$\left\{\frac{j_H/[(\sigma)_0 + \Delta\sigma]}{(j_N)_0/(\sigma)_0}\right\}^2 = \omega^2\tau^2\left[\frac{\Delta\sigma}{(\sigma)_0 + \Delta\sigma}\right]^2 \tag{7}$$

Equations (6) and (7) indicate that at high $\omega\tau$ an increase in conductivity of a stream tube will be accompanied by a (reversed) flow of Hall current, a resultant increase in electron temperature, which further increases the conductivity, and so on. Observe that it only takes a conductivity perturbation $\Delta\sigma/(\sigma)_0 > 1/\omega\tau$ to make $|j_H| > |(j_N)_0|$. Under nonequilibrium conditions the frequent occurrence of a perturbation of such magnitude seems more than likely.

Also, observe that this effect seems more powerful than the "thermal pinch" that constricts an ordinary arc. In the latter, the feedback mechanism that favors a higher electron temperature in a region of higher conductivity is the reduced atom density and increased atom temperature resulting from the higher Joule dissipation in that region.

On the other hand, this analysis does not take into account loading of the generator, or the $\mathbf{j} \times \mathbf{B}$, and convective forces, all of which would tend to stabilize or break up a spoke or longitudinal streamer. However, in our present small experiment, and at Mach numbers of around 0.7, the convection and $\mathbf{j} \times \mathbf{B}$ forces are not very large.

When a movie camera was set up looking edgewise into the disk, the resulting color films showed regions of blue-white color (as compared to the generally red or violet color of the rest of the gas) which, in at least some cases, were clearly in the form of a spoke or spokes extending from the inner to the outer electrode rings. These moved about and were difficult to see on a black and white still picture. However, the more intense spoke, produced by connecting a battery and driving a heavy reversed flow of Hall current through the generator, could be seen easily. Figure 12 is an example.

The spokes always appeared as the Hall current was decreased below the shoulder of the *V-I* trace. When the initial electron density was low, their appearance was frequently accompanied by an abrupt drop in output voltage of 10 to 20%, but when the initial electron density was high, this abrupt drop was not observed.

In an effort to prevent spoke formation, the outer electrode ring was split into 30 separate electrodes, each connected to the inner ring through separate variable resistors, all of which were ganged so that they could be turned up and down together. In principle a spoke should have more trouble establishing and maintaining itself if it can draw power from only a limited portion of the generator. However, in fact, relatively little difference was observed in the behavior of the generator and of the spokes. This is not easy to understand. It suggests either that 30 separate spokes occurred, which for the most part were too faint to be seen, or on the other hand, that the spokes are not really suppressing our output very much but perhaps only contribute to making it noisy.

Increased ionization in the vicinity of Hall current short circuit that is below the knee of the *V-I* curve, should result in an increase in the slope of the *V-I* characteristic there. The relative change can be measured by comparing the measured open-circuit voltage and the *V* axis intercept of the tangent to the *V-I* curve near short circuit. The procedure and results are given in Fig. 11 for a range of initial electron densities (as indicated by the range of short-circuit Hall currents). For these experiments, the calculated value of the ideal open-circuit Hall voltage (length $\times$ $[\omega\tau UB]$) is about 65 v (i.e., assuming equilibrium conductivity and a perfectly uniform gas). The measured open-circuit voltages show a slight tendency to decrease with increasing short-circuit current while the extrapolated voltages tend to increase. These trends are consistent with achieving a greater degree of nonequilibrium ionization for the higher current runs. Note that the largest extrapolated values of Hall voltage occurred when the outer electrode ring was "segmented" into 30 separate electrodes. However, in view of the scatter of the data it is hard to say whether only two points are statistically significant.

IV. Summary

A. Straight Channels

As measured by the generated Hall voltages, the performance of straight, segmented-electrode channels using an inert gas was poor. At Hall parameters ($\omega\tau$) of 5 to 15 and very fine segmenting, it was not possible to generate Hall fields much greater than twice *UB*. The poor performance appeared to be due to a nonuniformity created by nonequilibrium ionization over the electrode walls. However, a theoretical investigation by Kerrebrock suggests the existence of a stability boundary within which improved performance might be obtained. Experiments, partially motivated by this theory, are in progress.

B. Disk Channel

Nonequilibrium ionization and enhancement of the power output due to $\mathbf{U} \times \mathbf{B}$ ionization appears to have occurred

and to have done so under conditions that correspond very well with what one would predict on the basis of electric field experiments and of theory if the effects of radiation are included. The experiments were done at a pressure, temperature, and ionization level sufficiently close to what is likely to be encountered in practice, so that we can be reasonably confident that the atomic processes that dominate in the experiment are the same ones that would do so in a practical machine. A partial exception to this is the radiation loss. However, this only goes down as the square root of the linear dimension, or roughly the fourth root of the gas flow rate.

Perhaps the most significant result of this work is just the demonstration of an ability to run at high $\omega\tau$ with ionization frozen at the stagnation level (about 10 times the local equilibrium value at Mach 0.7). This proved stable on the scale of the present experiment; and the conductivity at which we ran (about 10 mho/m) could in fact be adequate for commercial nuclear applications of the MHD generator.

Appendix

Sensitivity of Measurements at High $\omega\tau$ to the Presence of Nonuniformties

The most damaging and also one of the most likely nonuniformities consists of a variation of conductivity in the $\mathbf{U} \times \mathbf{B}$ or the "normal current" direction. In this case, Ref. 3 shows that the equations of current flow (neglecting ion slip) become

$$j_H = \sigma E_H + \omega\tau j_N \tag{A1}$$

$$j_N = (\sigma/G)(UB + E_N) - (\omega\tau/G)\, j_H \tag{A2}$$

where E_H and j_H are the Hall components, E_N and j_N are the normal components of field and current, and

$$G = \langle\sigma\rangle_{av}\langle 1/\sigma\rangle_{av} + (1 - \langle\sigma\rangle_{av}\langle 1/\sigma\rangle_{av})\omega^2\tau^2 \tag{A3}$$

where G is the $\omega\tau$ dependent function that introduces the effects of nonuniformity. The brackets $\langle\ \rangle_{av}$ denote averages. It will also be convenient to have the inverted forms of Eqs. (1) and (2)

$$j_H = \frac{\sigma}{1 + (\omega^2\tau^2/G)}\left[E_H + \frac{\omega\tau}{G}(UB + E_N)\right] \tag{A4}$$

$$j_N = \frac{\sigma}{G + \omega^2\tau^2}[(UB + E_N) - \omega\tau E_H] \tag{A5}$$

Now the simplest and most informative measurements are those of open-circuit voltage and short-circuit current measured both when the orthogonal component is shorted and open. In general the measured values will be least accurate if they are a strong function of G and most accurate if they are a weak function or independent of G.

The normal component of current that results when the Hall circuit is open will be denoted by $j_N(0)$, and when the Hall current is shorted by $j_N(s)$. The other quantities of interest will be denoted in similar fashion. Hence, putting j_H and $E_N = 0$ in Eq. (2) yields

$$j_N(0) = (\sigma/G)UB \ldots \text{(inaccurate)} \tag{A6}$$

Putting E_H and $E_N = 0$ in Eq. (5) yields

$$j_N(s) = \frac{\sigma UB}{G + \omega^2\tau^2} \ldots \text{(moderately accurate)} \tag{A7}$$

because in general $G = \omega^2\tau^2$ times a number small compared to one. Putting j_N and $j_H = 0$ in Eq. (2) yields

$$E_N(0) = UB \ldots \text{(accurate)} \tag{A8}$$

and, putting E_H and $j_N = 0$ in Eq. (5) yields

$$E_N(s) = UB \ldots \text{(accurate)} \tag{A9}$$

Now for the Hall components

$$j_H(0) = 0 \ldots \text{(accurate)} \tag{A10}$$

From Eq. (4) for $E_N = 0$,

$$j_H(s) = \frac{\omega\tau\sigma UB}{G + \omega^2\tau^2} \ldots \text{(moderately accurate)} \tag{A11}$$

from Eq. (1),

$$E_H(s) = 0 \ldots \text{(accurate)} \tag{A12}$$

and from Eq. (4) for $E_N = 0$,

$$E_H(0) = (\omega\tau/G)UB \ldots \text{(inaccurate)} \tag{A13}$$

Of the preceding, Eqs. (8–10) and (12) are essentially trivial and Eqs. (6) and (13) are inaccurate. This leaves Eqs. (7) and (11) as the measurements yielding the most interesting and reasonably accurate information. Assuming that $\omega^2\tau^2 \gg 1$, Eq. (11) yields

$$j_H(s) = (\sigma UB/\omega\tau) = n_e eU \tag{A14}$$

where n_e and e are the electron density and charge. Hence, assuming U is well known from conventional gasdynamic measurements, a measurement of short-circuit Hall current gives a reasonably accurate measurement of electron density.

Division of Eq. (11) by Eq. (7) yields another quantity of interest, namely $\omega\tau$, or assuming B is known, the electron mean free time τ, i.e.

$$[j_H(s)/j_N(s)] = \omega\tau \tag{A15}$$

Although Eq. (14) gives a good measure of electron density in a shorted Hall generator, we would like also to measure electron density in an open-circuit Hall generator because this is the condition under which nonequilibrium ionization is most likely to occur. Division of Eq. (6) by Eq. (13) yields

$$j_N(0)/E_H(0) = \sigma(\text{hot})/\omega\tau = n_e(\text{hot})e/B \tag{A16}$$

in which n_e ("hot electron") appears, but G does not. If G or the variation of σ with position and time was fixed, then this should be a reasonably accurate measurement. However, it is of course the nature of imperfections to be imperfect, i.e., vary in more or less unpredictable fashion. In particular it is altogether likely that, when extrathermal ionization occurs, $G(0)$ is significantly different from $G(s)$.

Of course none of these measurements are accurate unless electrode drops are small and short circuits are truly short. This can be difficult to arrange, especially at high $\omega\tau$. However, if probes are placed in the channel away from the electrodes, the residual fields in the gas can be measured and used to correct the calculations. For example, we have obtained seemingly good accuracy by using instead of Eq. (15) the expression obtained from Eqs. (4) and (5)

$$\omega\tau = \frac{j_H(s)}{j_N(s)} \cdot \left[\frac{1 + (E_N/UB) - \omega\tau(E_H/UB)}{1 + (E_N/UB) + (G/\omega\tau)(E_H/UB)}\right]$$

or since it is usually all too easy to make

$$[E_H/(\omega\tau UB)] \ll 1$$

the term involving G drops out and the expression can be rearranged to yield

$$\omega\tau = \frac{j_H(s)}{j_N(s)} \cdot \frac{1 + E_N/UB}{1 + E_N/UB + [j_H(s)/j_N(s) \cdot E_H/UB]} \tag{A17}$$

where E_N and E_H are the residual fields remaining after the Hall and normal electrodes are shorted out.

References

[1] Louis, J. F., Lothrop, J., and Brogan, T. R., "Fluid dynamic studies with a magnetohydrodynamic generator," Phys. Fluids **7**, 362–374 (1964).

[2] Rosa, R. J., "Nonequilibrium ionization in MHD generators," Proc. Inst. Elec. Electron Engrs. **51**, 774–784 (1963).

[3] Rosa, R. J., "The Hall and ion slip effects in a nonuniform gas," Phys. Fluids **5**, 1081–1090 (1962).

[4] Klepeis, J., "Graphite heater for MHD studies," Rev. Sci. Inst. **35**, 846–847 (1964).

[5] Carlson, A. W., "A Hall generator with wire electrodes," Avco-Everett Research Lab. Research Rept. 165 (September 1963).

[6] Hurwitz, H., Jr., Kilb, R. W., and Sutton, G. W., "Influence of tensor conductivity on current distribution in an MHD generator," J. Appl. Phys. **32**, 205–216 (1961).

[7] Kerrebrock, J. L., "Segmented electrode losses in MHD generators with nonequilibrium ionization," Avco-Everett Research Lab. Research Rept. 178 (1964).

[8] Kerrebrock, J. L., "Segmented electrode losses in MHD generators with nonequilibrium ionization," Avco-Everett Research Lab. Rept. 201 (December 1964); also *6th Symposium on the Engineering Aspects of MHD* (University of Pittsburgh, Pittsburgh, Pa., 1965).

[9] Klepeis, J. and Rosa, R. J., "Experimental studies of strong Hall effects and $\mathbf{U} \times \mathbf{B}$ induced ionization—II," *6th Symposium on the Engineering Aspects of MHD* (University of Pittsburgh, Pittsburgh, Pa., 1965).

[10] Bates, D. R., Kingston, A. E., and McWhirter, R. W. P., "Recombination between electron and atomic ions I. optically thin plasmas," Proc. Roy. Soc. (London) **A267**, 297–312 (1962).

[11] Byron, S., Stabler, R. C., and Bortz, P. I., "Electron-ion recombination by collisional and rediative processes," Phys. Rev. Letter **8**, 376–379 (1962).

[12] Makin, B. and Keck, J. C., "Variational theory of three-body electron-ion recombination rates," Phys. Rev. Letters **11**, 281 (1963).

[13] Velichov, E. P., *Proceedings Symposium on MPD Electric Power Generation* (University of Durham, Newcastle upon Tyne, England, 1962), pp. 6–8.

[14] McCune, J. E., "Instability in MHD plasmas," Avco-Everett Research Lab. Research Report Avco Miscellaneous Publ. 136 (April 1964).

[15] Kerrebrock, J. L. and Hoffman, M., "Nonequilibrium ionization due to electron heating, Part II—experiments," AIAA J. **2**, 1080–1087 (1964).

[16] Lutz, M. A., "Radiant energy loss from a cesium-argon plasma to an infinite plane-parallel enclosure," Avco-Everett Research Lab. Research Rept. 175 (September 1963).

SEPTEMBER 1965 AIAA JOURNAL VOL. 3, NO. 9

Rendezvous Problem for Nearly Circular Orbits

MAURICE L. ANTHONY* AND FRANK T. SASAKI†
Martin Company, Denver, Colo.

In order to assess various closure techniques during the terminal phase of a rendezvous maneuver, it is desirable to know the free flight motion of one vehicle relative to another. When expressed in terms of a reference system centered at the target vehicle, the equations of motion that are to be solved are a set of nonlinear differential equations with explicit time-dependent coefficients. In this paper an approximate analytical solution is determined by utilizing perturbation techniques. The solution is more general than those previously found since it includes the case where the target orbit possesses small eccentricity, and it remains valid for relatively large distances between the vehicles. Hence the results are useful for many near-earth missions. Numerical examples are provided in order to assess the accuracy of the solution. The results indicate that in certain instances the present solution, which includes some non-linear effects, must be used in lieu of previous solutions that are based on a linear theory. An approximate analytical solution is also obtained by which the required velocity components can be determined in order to effect rendezvous at a prescribed time.

Nomenclature

a_T, e, M = semimajor axis, eccentricity, and mean anomaly of target orbit
$\bar{R}$ = relative position vector to interceptor ($\bar{R}_I - \bar{R}_T$)
$\bar{R}_I, \bar{R}_T$ = inertial position vectors to interceptor and target vehicles
t, t_p = time, and time of periapsis passage
$\bar{V}$ = relative velocity of interceptor
x, y, z = nondimensional coordinates
X, Y, Z = coordinates of interceptor relative to target
$\delta z, \delta y, \delta z$ = variations of nondimensional coordinates from Clohessy-Wiltshire results
θ, ω = angular coordinate and angular speed of target vehicle
μ = gravitational constant
ρ = R_T/a_T
τ = $(\mu/a_T^3)^{1/2}t$
τ^* = specified nondimensional time to rendezvous
φ = angle denoting direction of initial velocity difference, measured from the X axis

Subscripts

c = associated with solution to linearized equations of motion, target in circular path
0 = denotes conditions at $t = 0$

Superscripts

$(\cdot), (\ )'$ = derivatives with respect to t and τ, respectively
$0, e$ = indices used in identifying coefficients in the solution

Presented as Preprint 65-32 at the AIAA 2nd Aerospace Sciences Meeting, New York, January 25–27, 1965; revision received May 3, 1965. The authors gratefully acknowledge the assistance of Dale E. Chambers, of Martin-Co., Denver, Colo., in providing the numerical results and preparing the figures for this paper.

* Manager, Astrodynamics Staff. Associate Fellow Member AIAA.

† Associate Research Scientist. Member AIAA.